A Land Surface Process/Radiobrightness Model with Coupled Heat and Moisture Transport for Prairie Grassland

Yuei-An Liou, *Member, IEEE,* John F. Galantowicz, *Member, IEEE,* and Anthony W. England, *Fellow, IEEE*

***Abstract*—We present a biophysically based, one-dimensional hydrology/radiobrightness (1dH/R) model for prairie grassland that is subject to solar heating, radiant heating and cooling, precipitation, and sensible and latent heat exchanges with the atmosphere. The 1dH/R model consists of two modules, a one-dimensional hydrology (1dH) module that estimates the temperature and moisture profiles of the soil and the canopy and a microwave emission module that predicts radiobrightness (R).**

We validate the 1dH/R model by comparing its predictions with data from a field experiment. The model was forced by meteorological and sky radiance data from our Radiobrightness Energy Balance Experiment (REBEX-1) on prairie grassland near Sioux Falls, SD, during the fall and winter of 1992–1993. Model predictions were compared with 995 consecutive REBEX-1 observations over a 14-day period in October. Average errors (predicted-measured) for canopy temperature are 1.1 K with a variance of 3.72 K^2, for soil temperatures at 2-, 4-, 8-, 16-, 32-, and 64-cm depths are 2 K with a variance of 4 K^2, and for H-polarized brightnesses are 0.06 K with a variance of 1.30 K^2 at 19 GHz and 6.01 K with a variance of 6.04 K^2 at 37 GHz. The model overestimates the 37-GHz brightness because we have not included scatter darkening within the vegetation canopy in the model.

We use the 1dH/R model to simulate a 60-day dry-down of prairie grassland in summer. For grass with a column density of 3.7 kg/m^2 and soil with an initially uniform moisture content of 38% by volume, the upper 5 mm of soil dries to 27% by the end of the simulation. The corresponding L-band brightness increases from an initial 143 K to a final 163 K. In contrast, none of the special sensor microwave/imager (SSM/I) radiobrightnesses nor the radiobrightness thermal inertia (RTI) technique, either at L-band or at any SSM/I frequency, exhibits significant sensitivity to the soil dry-down.

I. Introduction

SOIL moisture affects the energy budget at the land-atmosphere interface, primarily through its influence on the exchange of latent energy. Soil moisture is conveniently described by two measures: 1) surface soil moisture—water in the liquid state that is found in the upper 5 cm of soil—and 2) stored water—water (vapor, liquid, or ice) in soil, snow, or vegetation that is available to the atmosphere through diffusion, evaporation, transpiration, or sublimation, as appropriate. Stored water will be found on and in vegetation, as snow or ice, and within the upper meter or so of soil. Surface soil moisture is roughly the soil moisture that can be sensed by microwave techniques. Stored water is a hydrologic concept defined by land–atmosphere moisture transport processes. Maintaining an estimate of soil moisture is an essential task of the land surface process (LSP) models that are part of weather and climate models. Errors in the estimate of either surface soil moisture or stored water contribute to errors in estimates of latent energy flux and, finally, to potentially significant errors in model-based predictions about weather or near-term climate [1]–[3].

The biosphere–atmosphere transfer scheme (BATS) [4], the simple biosphere model (SiB) [5], and the simplified biosphere model (SSiB) [6] are examples of commonly used LSP models. The computational requirement that LSP models interact at each time step with all of the near-surface grid points of an atmospheric model has led to highly parameterized characterizations of the physical processes that occur at the land–atmosphere interface. Most parameterizations within operational LSP models have been empirically tuned to yield an atmosphere whose behavior is consistent with observations. The parameterization for the equivalent of soil moisture may not represent an observable in the field.

LSP moisture estimates could be improved by the assimilation of observational data, much as state estimates within atmospheric models are improved by the assimilation of observed atmospheric temperature and humidity profiles. Radiobrightnesses at lower microwave frequencies are known to be sensitive to surface soil moisture [7]–[11], and they would be candidates for assimilation if there were reliable relationships between surface soil moisture and the moisture parameterizations of the LSP models [12], [13]. Our approach to establishing this relationship has been to substitute a one-dimensional hydrology (1dH) model for the LSP model, predict radiobrightness (R) based on the soil moisture and temperature profiles of the 1dH model, and use the difference between observed and predicted radiobrightness as a measure of error in the 1dH model's estimate of stored water. The power of the approach has been demonstrated for bare soils [14]–[16]. A similar approach has been used by Mahfouf [17]

Manuscript received February 27, 1997; revised November 6, 1998. This work was supported by NASA under Grant NAGW 3430, and the National Science Council under Grant NSC87-2111-M-008-221.

Y.-A. Liou is with the Center for Space and Remote Sensing Research, National Central University, Chung-Li, Taiwan, R.O.C. (e-mail: yueian@csrsr.ncu.edu.tw).

J. F. Galantowicz was with the Department of Civil and Environmental Engineering, Massachusetts Institute of Technology, Cambridge, MA 02139 USA. He is now with Atmospheric and Environmental Research, Inc., Cambridge, MA 02139 USA (e-mail: johng@aer.com).

A. W. England is with the Department of Electrical Engineering and Computer Science, The University of Michigan, Ann Arbor, MI 48109-2122 USA (e-mail: england@umich.edu).

Publisher Item Identifier S 0196-2892(99)05002-0.

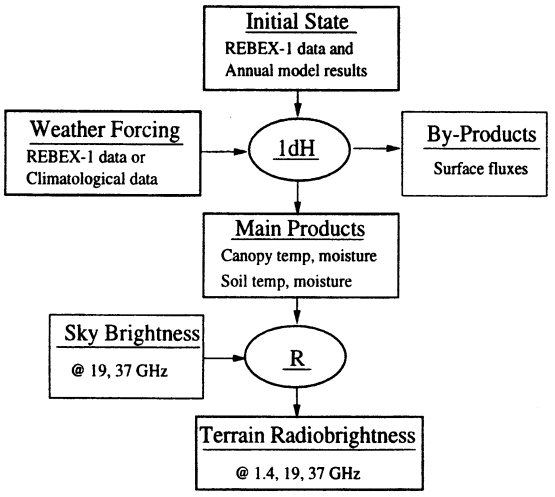

Fig. 1. Schematic diagram of the 1dH/R model inputs and products.

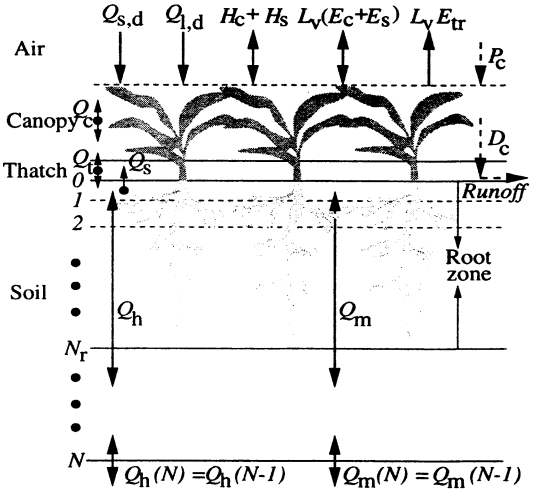

Fig. 2. A 1dH module schematic diagram of land–air interactions for vegetated fields.

and Bouttier *et al.* [18], except that they assimilated local weather observations to improve point estimates of stored water. Lakshmi *et al.* present a soil–canopy-atmosphere model for use in satellite microwave remote sensing [19]. They treat the soil as a two-layer system, much like BAT's or SiB.

In this paper, we present a 1dH/R model of prairie grassland that is based on a combination of our bare-soil model and a biophysical and radiative transfer model of the grass canopy. The new model is validated with observations from our Radiobrightness Energy Balance Experiment (REBEX-1) in prairie grassland near Sioux Falls, SD, during the fall and winter of 1992–1993 [20]. The model is then used to simulate a 60-day dry-down of grass-covered prairie in summer. Our objective is to examine the sensitivity of various radiobrightness frequencies and techniques for remotely measuring soil moisture in prairie grassland.

II. 1dH/R Model

A. Overview

The 1dH/R model consists of two modules: a 1dH module and a radiobrightness (R) module. Fig. 1 is a schematic diagram of the 1dH/R model inputs and products. The 1dH module simulates the LSP's and estimates temperature and moisture profiles in soil and canopy for grass-covered fields. Assigned grass coverage may vary from 0% to 100%. The R module is a radiative transfer model similar to that developed by England and Galantowicz [21]. The soil is modeled as in Liou and England [15], [16], except that we account for the effects of transpiration on energy and moisture within the root zone.

The canopy is divided into two layers. The top layer links the soil and atmosphere through dynamic exchanges of energy and moisture, and the bottom layer, a thin insulating layer of thatch, is subject to radiant energy exchanges with the top layer, atmosphere, and underlying soil.

B. 1dH Module

A schematic diagram of the 1dH module land–air interactions for vegetated soils is shown in Fig. 2. The vegetated field is subject to solar heating $Q_{s,d}$, radiant heating from the sky $Q_{l,d}$, radiant cooling of the canopy Q_c and of the bare soil Q_s, sensible heat exchanges with the air from the canopy H_c and from the soil H_s, evaporative heat loss from the wet foliage L_vE_c and from the bare soil L_vE_s, heat loss due to transpiration L_vE_{tr}, and heat exchange through precipitation, P_c. The other parameters in Fig. 2 are gray-body emission from the thatch Q_t and from the soil Q_s, energy flux Q_h, and moisture flux Q_m within the soil, drainage from the canopy D_c, runoff at the soil–canopy interface Rr, total number of soil layers N, and number of soil layers within the root zone N_r.

The coupled transfer of energy and moisture governs the temperature and moisture profiles of the soil and canopy. The next sections describe details of the modeling of the upper canopy layer (canopy), lower canopy layer (thatch), soil layers, and fluxes.

1) Canopy Layer: For the canopy layer, equations for the conservation of energy and moisture are

$$\frac{\partial X_{hc}}{\partial t} = F_c \tag{1}$$

$$\frac{\partial X_{mc}}{\partial t} = \rho_l(P_c - D_c - E_c) \tag{2}$$

respectively, where

$X_{hc} = (W_c c_c + W_l c_l)(T_c - T_0)$ total heat content per unit area of the canopy layer, J/m^2:

W_c dry canopy mass kg/m^2;
W_l canopy moisture mass kg/m^2;
c_c canopy specific heat (typical = 2700 [22]) J/kg-K;
c_l specific heat of liquid water at constant pressure J/kg-K;
T_c canopy temperature K;
T_0 reference temperature K;

$X_{mc} = W_l = W_{ls} + W_r$ is the total moisture per unit area of the canopy layer, kg/m^2:

W_{ls} static moisture content in the canopy kg/m^2;
W_r moisture stored on the foliage, kg/m^2;
t time s;

$F_c = R_{\rm nc} - H_c - \rho_l L_v E_{tr} - \rho_l L_v E_c$ is a function of the energy balance components of the canopy layer, W/m^2:

$R_{\rm nc}$ net radiation absorbed by the canopy, W/m^2;
H_c sensible heat flux between the atmosphere and canopy, W/m^2;
L_v latent heat of vaporization of water, J/kg;
E_{tr} rate of transpiration from the dry fraction of the canopy, m/s;
E_c rate of vaporization from the wet fraction of the canopy, m/s;
ρ_l density of liquid water, kg/m;^{3};
P_c rate of precipitation, m/s;
D_c rate of water drainage, m/s;
E_c rate of vaporization, m/s.

2) Thatch Layer: The thatch is a 2-cm layer of organic matter, like dead grass, that lies at the base of the grass canopy. It is subject to radiant heat exchange with the atmosphere, canopy layer, and underlying soil layers. Its energy budget is given by

$$\frac{\partial X_{\rm ht}}{\partial t} = F_t \tag{3}$$

where

$X_{\rm ht} = W_t c_t (T_t - T_0)$ the total heat content per unit area of the thatch, J/m^2
$W_t = r_{\rm tc} W_{\rm wc}$ mass of the thatch, kg/m^2;
$r_{\rm tc}$ ratio of the bottommost 2-cm wet biomass to the total wet biomass of the canopy (2 cm is chosen so that $r_{\rm tc}$ can be estimated using field observations given latter);
$W_{\rm wc} = W_c + W_{ls} + W_t$ mass of the wet canopy, kg/m^2;
c_t specific heat of the thatch, J/kg-K;
T_t thatch temperature, K;
$F_t = R_{\rm nt}$ is a function of the thatch energy balance components, W/m^2
$R_{\rm nt}$ net radiation absorbed by the thatch, W/m^2.

The value of the parameter $r_{\rm tc}$ was obtained from a field study of the vertical distributions of biomass and moisture in a grass canopy at The University of Michigan's Matthaei Botanical Garden by Dahl *et al.* [23]. The wet biomass was measured with 2-cm vertical resolution. The wet biomass of the grass at the REBEX-1 site was about 2.3 times the wet biomass of the grass at the Matthaei site.

3) Soil Layers: Energy and moisture conservation equations within the soil are (e.g., Liou and England [15], [16])

$$\frac{\partial X_h}{\partial t} = -\nabla \cdot \vec{Q}_h \tag{4}$$

$$\frac{\partial X_m}{\partial t} = -\nabla \cdot \vec{Q}_m \tag{5}$$

respectively, where

X_h total heat content per unit volume, J/m^3;
X_m total moisture content per unit volume, kg/m^3;
$\vec{Q}_m = \vec{Q}_v + \vec{Q}_l$ vector moisture flux density, kg/m^2-s, where $\vec{Q}_v$ and $\vec{Q}_l$ are the vector vapor and liquid flux densities, respectively;
$\vec{Q}_h$ vector heat flux density, J/m^2-s.

This current version of the soil module has been improved by incorporating the effect of transpiration on the moisture flux and on the energy flux within the root zone, i.e.,

$$\vec{Q}_l = \vec{Q}_{l,b} - \rho_l E_{tr} \hat{k} \tag{6}$$

where

$\vec{Q}_{l,b}$ vector liquid water flux for bare soil given by Liou and England [16], kg/m^2-s;
$\hat{k}$ vertical unit vector.

The boundary conditions on energy and moisture fluxes at the soil–canopy interface (upper) and with soils below the modeled column (lower) are required to solve (4) and (5). The lower boundary is chosen to be at a depth unaffected by diurnal thermal and moisture variations so that energy and moisture fluxes are constant (see Fig. 2), i.e.,

$$Q_h(N) = Q_h(N-1) \tag{7}$$

$$Q_m(N) = Q_m(N-1) \tag{8}$$

where

N the number of soil layers;
$Q_h(N)$ heat flux density at the Nth layer boundary, J/m^2-s, from our annual model for day-of-year;
Q_m moisture flux density at the Nth layer boundary, kg/m^2-s.

At the upper boundary, the energy and moisture fluxes are

$$\vec{Q}_h(0) = R_{\rm ns} - H_s - \rho_l L_v (E_s + E_{tr}) \tag{9}$$

$$\vec{Q}_m(0) = \rho_l (D_c - E_s - E_{tr} - Rr) \tag{10}$$

respectively, where

$R_{\rm ns}$ net radiation absorbed by the soil, W/m^2;
H_s sensible heat flux from bare soil, W/m^2;
E_s rate of evaporation from bare soil, m/s;
Rr rate of runoff, m/s.

4) Radiation Fluxes: Longwave and shortwave radiation transfer occur among the vegetation, thatch, and soil. Shortwave radiation is described by the nonscattering Beer's law of radiative transfer so that the transmissivity of shortwave radiation for the canopy becomes [22]

$$\tau_c = \exp(-\kappa_c {\rm LAI}) \tag{11}$$

where

κ_c extinction coefficient of the canopy (=0.4/ cos Z for crops and grass);
LAI leaf area index, m^2/m^2;
Z solar zenith angle, degrees.

Similarly, the transmissivity of shortwave radiation for the thatch is

$$\tau_t = \exp(-\kappa_c \mathrm{LAI}_t) \tag{12}$$

where $\mathrm{LAI}_t = r_{tc}\mathrm{LAI}$ is the leaf area index of thatch, m^2/m^2.

The net radiation absorbed by the canopy and by the thatch layers is

$$R_{nc} = \mathrm{veg}[(1-\tau_c)(1-A_c)Q_{s,d} + e_c Q_{l,d} + e_c e_t \sigma T_t^4 - 2e_c \sigma T_c^4] \tag{13}$$

$$R_{nt} = \mathrm{veg}[\tau_c(1-A_c)(1-A_t)(1-\tau_t)Q_{s,d} + e_t e_c \sigma T_c^4 + e_t e_s \sigma T_s^4 - 2e_t \sigma T_t^4] \tag{14}$$

respectively, where

veg fraction of the canopy cover;
A_c albedo of the canopy;
A_t albedo of the thatch;
$Q_{s,d}$ downwelling shortwave radiation, W/m^2;
$Q_{l,d}$ downwelling longwave radiation, W/m^2;
e_c emissivity of the canopy;
e_t emissivity of the thatch;
e_s emissivity of the soil;
σ Stefan–Boltzmann constant, $W/m^2\text{-}K^4$;
T_c canopy temperature, K;
T_t thatch temperature, K;
T_s soil temperature (top layer), K.

The following four terms between the brackets of (13) represent:

1) absorbed shortwave radiation corrected by the transmissivity and albedo of the canopy;
2) absorbed downwelling sky thermal radiation;
3) absorbed thermal emission from the underlying thatch;
4) gray-body emission from the canopy in both upward and downward directions.

The four terms between the brackets in (14) are the absorbed shortwave radiation, the absorbed canopy thermal emission, absorbed soil thermal emission, and thermal emission of the thatch, respectively.

The net radiation absorbed by the soil is

$$R_{ng} = \mathrm{veg}\left[e_s e_t \sigma T_t^4 + \tau_c \tau_t (1-A_c)(1-A_t)(1-A_s)Q_{s,d}\right] + (1-\mathrm{veg})[(1-A_s)Q_{s,d} + e_s Q_{l,d}] - e_s \sigma T_s^4 \tag{15}$$

where A_s is albedo of the soil. Between the first set of brackets, the first term is the downwelling thermal emission absorbed from the thatch and the second term is the downwelling shortwave radiation modified by the transmissivity and albedo of both the thatch and the canopy and by the albedo of the soil. The two terms between the second set of brackets are the shortwave and longwave radiation absorbed by the bare soil, respectively. The last term of the equation is gray-body emission from the soil.

5) Sensible and Latent Heat Fluxes:

Sensible heat transfer: Sensible heat exchanges between the atmosphere and the vegetation and the atmosphere and the soil are modeled with the bulk aerodynamic approach [24]

$$H_c = \mathrm{veg}\rho_a c_{p,a} \frac{T_c - T_{a,r}}{r_{ac}} \tag{16}$$

$$H_s = (1-\mathrm{veg})\rho_a c_{p,a} \frac{T_s - T_{a,r}}{r_{as}} \tag{17}$$

respectively, where

ρ_a air density, kg/m^3;
$c_{p,a}$ specific heat of air, J/kg-K;
r_{ac} aerodynamic resistance between the atmosphere and canopy, s/m;
r_{as} aerodynamic resistance between the atmosphere and bare soil, s/m;
$T_{a,r}$ temperature of the air at the first reference height (1.8 m), K.

The aerodynamic resistance is described by [25]

$$r_{ax} = \frac{\{\ln[(z_{r2} - d + z_0)/z_0]\}^2}{k^2 u_{r2}} \tag{18}$$

where

ax ac (air-canopy) or as (air-soil);
z_{r2} second reference height (=10), m;
z_0 surface roughness (=0.028 h_c for the prairie [26]; =0.015 for bare soil), m;
d zero plane displacement (=0.71 h_c for the prairie [26]; negligible for bare soil), m;
h_c canopy height (=0.6), m;
u_{r2} wind speed at the second reference height, m;
k Von Karman's constant (=0.4).

Latent heat transfer—Evaporation and condensation: Evaporation occurs from soil and the fraction of foliage that is covered by a film of water, while transpiration occurs from the fraction of foliage that is dry. The fraction of the foliage covered by a film of water is given by [5]

$$\delta_w = \frac{W_r}{W_{r,\max}}, \quad \text{if } e_{\mathrm{sat}}(T_c) > e_a$$
$$= 1, \quad \text{otherwise} \tag{19}$$

where

$W_{r,\max} = (0.2 \sim 0.5)$ LAI [5] maximum stored moisture on the foliage, kg/m^2;
$e_{\mathrm{sat}}(T_c)$ saturation water vapor pressure at T_c, Pa;
e_a atmospheric water vapor pressure, Pa.

Evaporation from the canopy and soil are described by

$$\rho_l L_v E_c = \mathrm{veg} L_v \rho_a \frac{q_{\mathrm{sat}}(T_c) - q(T_a)}{r_{ac}} \delta_w \tag{20}$$

$$\rho_l L_v E_s = (1-\mathrm{veg}) L_v \rho_a \times \frac{\mathrm{RH}_s q_{\mathrm{sat}}(T_s) - q(T_a)}{r_{as}} \tag{21}$$

respectively, where

$q_{\mathrm{sat}}(T_c)$ saturation specific humidity at T_c;
$q(T_a)$ atmospheric specific humidity at T_a;
RH_s relative humidity of the first soil layer.

The relative humidity is given by [27]

$$\mathrm{RH}_s = \exp(-\Psi g/RT_s) \tag{22}$$

where

Ψ suction of the first soil layer, m;
g acceleration due to gravity, m/s^3;
R gas constant of water vapor, J/kg-K.

Equations (20) and (21) also describe condensation, which occurs when evaporation ceases.

Latent heat transfer—Transpiration: Transpiration is modeled as

$$\rho_l L_v E_{tr} = \mathrm{veg} L_v \rho_a \frac{q_{\mathrm{sat}}(T_c) - q(T_a)}{r_{\mathrm{ac}} + r_c}(1 - \delta_w) \tag{23}$$

where r_c is canopy resistance, s/m. Transpiration stops if the air temperature is lower than the freezing point or if condensation occurs. The canopy resistance is primarily affected by incoming solar radiation, the air vapor pressure deficit, soil moisture (matric head), and air temperature [28], i.e.,

$$r_c = \frac{r_{c,\min}}{\mathrm{LAI} F_1(Q_{s,d}) F_2(\theta_l) F_3(q_{\mathrm{sat}}) F_4(T_a)} \tag{24}$$

where $r_{c,\min}$ is the minimum canopy resistance, s/m, and θ_l is the water content volume fraction.

The fractional parameters F_x, $x = 1, \cdots, 4$ are defined as follows [28]:

$$F_1 = \frac{r_{c,\min}/r_{c,\max} + f}{1 + f} \tag{25}$$

$$F_2 = \min(1, 40/\Psi_{s,r}) \text{ [22]} \tag{26}$$

$$F_3 = 1 - 0.06(q_{\mathrm{sat}}(T_a) - q_a), \quad \text{and} \quad F_3 \geq 0.33 \tag{27}$$

$$F_4 = 1 - 1.6 \times 10^3 \times (298 - T_a) \tag{28}$$

where

$r_{c,\max}$ maximum canopy resistance (=5000), s/m;
$f = 0.55 \frac{2Q_{s,d}}{\mathrm{LAI} Q_{sd1}}$ dimensionless term representing incoming photosythetically active shortwave radiation;
Q_{sd1} 30 W/m^2 for trees to 100 W/m^2 for crops [29];
$\Psi_{s,r}$ the minimum moisture suction of the soil layers within the rooting zone, m.

The amount of water extracted from the root zone due to transpiration is governed by the distribution of roots and the surrounding moisture profile. Similar to the approach of Verseghy *et al.* [22], we compute the fraction of extracted water from the ith soil layer using

$$F_{r,i} = \frac{\mathrm{Root}_i(\Psi_{\max,i} - \Psi_i)}{\sum_{i=1}^{N_r} \mathrm{Root}_i(\Psi_{\max,i} - \Psi_i)} \tag{29}$$

where

Root_i fractional root volume within the ith soil layer;
$\Psi_{\max,i}$ soil moisture suction corresponding to the wilting point at the ith soil layer;
Ψ_i soil moisture suction at the ith soil layer.

$\Psi_{\max,i}$ and Ψ_i are described by Liou and England [15], [16]. The fractional root volume below a given depth z is given by [22]

$$\mathrm{Root}(z) = \frac{\exp(-3z) - \exp(-3z_r)}{1 - \exp(-3z_r)} \tag{30}$$

where

z_r averaged canopy root depth (=0.3), m.

The fractional root volume within the ith soil layer is

$$\mathrm{Root}_i(z) = \mathrm{Root}(z_{i-1}) - \mathrm{Root}(z_i) \tag{31}$$

where z lies between z_{i-1} and z_i—the depths of the top and bottom of the soil layer, respectively.

6) Numerical Scheme: We use the numerical scheme developed by Liou and England [14], [15] to solve (1)–(5) for the temperatures and moisture contents of the soil layers and two canopy layers. As shown in Fig. 2, the soil profile is divided into N layers, including N_r layers in the root zone. We typically use 40 soil layers in our simulations. The thickness of the first layer is 5 mm, and the thicknesses of the other layers increase exponentially with depth. The time step varies with two factors, the speed of convergence and the strength of the weather forcings (solar heating and precipitation). For example, the time step may be about 15 s when there is no precipitation and solar radiation is less than 10 W/m^2. At other times, it may be assigned a value of 2–3 s.

C. The Radiobrightness Module

1) Dielectric Properties of Moist Soils: We estimate the dielectric properties of moist soils with a five-component mixture model of soil solids, air, free water, bound water, and ice. The dielectric properties are functions of temperature and moisture content/state. They were discussed in our previous work [14], [15] and will not be readdressed here.

2) Dielectric Properties and Optical Thickness of the Canopy: The relative permittivity of a wet canopy based on the dual-dispersion model of Ulaby and El-Rayes [30] is

$$\epsilon_{\mathrm{wg}} = \epsilon_r + v_{\mathrm{fw}}\left[4.9 + \frac{75}{1 + jf/18} - j\frac{18\sigma}{f}\right] + v_{\mathrm{bw}}\left[2.9 + \frac{55}{1 + (jf/0.18)^{0.5}}\right] \tag{32}$$

where

$\epsilon_r = 1.7 - 0.74 m_g + 6.16 m_g^2$ residual dielectric constant;
m_g gravimetric moisture constant of the wet grass, kg/kg;
$v_{\mathrm{fw}} = m_g(0.55 m_g - 0.076)$ volume fraction of free water in the grass;
$v_{\mathrm{bw}} = 4.64 m_g^2/(1 + 7.36 m_g^2)$ volume fraction of bound water in the grass;
$\sigma = 1.27$ ionic conductivity of the free water solution, S/m;
f frequency, GHz.

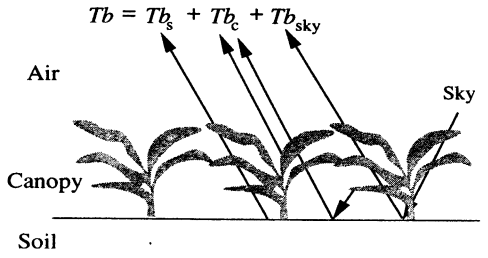

Fig. 3. Radiobrightness components of the 1dH/R model.

While the Ulaby and El-Rayes model was developed for corn leaves, we are unaware of a model that would be more suitable for grass. The total refractive index of the air-grass mixture layer can be approximated [21]

$$n_t = 1 + v_{\mathrm{wg}} n_{\mathrm{wg}} \tag{33}$$

where

$v_{\mathrm{wg}} = 9.26 \times 10^{-3} e^{-z/0.1149}$ volume fraction of the wet grass;

n_{wg} $\sqrt{\epsilon_{\mathrm{wg}}}$.

The optical thickness of the air-grass mixture layer is

$$\tau_0 = -\int_0^{\infty} 2k_0 \kappa \, dz \tag{34}$$

where

k_0 vacuum wavenumber, 1/m;

κ imaginary part of the total refractive index.

For a canopy layer of height h_c, (34) becomes

$$\tau_0 = 0.002\,212\,8 k_0 \sqrt{\epsilon_{\mathrm{wg}}} [e^{-h_c/0.1149} - 1]. \tag{35}$$

3) Emission Model: We used the emission model of England and Galantowicz [21]. As shown in Fig. 3, the total model brightness comprises four components: Tb_s, the soil brightness attenuated by one trip through the canopy; $Tb_{c,d}$, the downwelling canopy brightness reflected by the soil and attenuated by one trip through the canopy; $Tb_{c,u}$, the upwelling canopy brightness; and Tb_{sky}, the sky brightness reflected by the soil and attenuated by two trips through the canopy. That is

$$\begin{aligned} Tb_s &= T_{s,e}(1 - R_p(\mu))e^{-\tau_0/\mu} \\ Tb_{c,d} &= T_{c,e}(1 - e^{-\tau_0/\mu}) R_p(\mu) e^{-\tau_0/\mu} \\ Tb_{c,u} &= T_{c,e}(1 - e^{-\tau_0/\mu}) \\ Tb_{\mathrm{sky}} &= T_{\mathrm{sky}} R_p(\mu) e^{-2\tau_0/\mu} \end{aligned} \tag{36}$$

where

$T_{s,e}$ effective emitting temperature of the soil [14], [15], K;

R_p Fresnel reflectivity of the moist soil for polarization p;

μ cosine of the SSM/I incidence angle of 53°;

$T_{c,e}$ effective emitting temperature of the canopy, K.

To first order

$$T_{s,e}(t) = T_s(0,t) + \frac{1}{\kappa_e \sec\theta_t} \cdot \left(\frac{\partial T_s(z,t)}{\partial z} \right)_{z=0} \tag{37}$$

where κ_e is extinction of the soil, θ_t is a transmission angle, T_g is the soil temperature, and z is the depth, m. $T_{c,e}$ can be approximated as the average temperature of the two canopy layers

$$T_{c,e} = \frac{1}{2}(T_c + T_t). \tag{38}$$

III. Validation of Grassland Model

We validated the 1dH/R model by comparing model predictions with observations from REBEX1 for the 14 day period from day 287 (October 13, 1992) to day 300 (October 26, 1992). The grass was green and there was no snow cover. REBEX-1 was conducted on the grounds of the US. Geological Survey's EROS Data Center near Sioux Falls, South Dakota from October, 1992 through April, 1993. Measurements at half-hour intervals included horizontally polarized ground and sky brightnesses at the SSM/I frequencies and incidence angle of 53 degrees, soil temperatures at two locations for depths of 2, 4, 8, 16, 32, and 64 cm, soil heat flux at 2 cm depth, 10 m wind speed, air temperature at 1.8 m height, air relative humidity, down-welling shortwave radiation, net radiation, precipitation, and thermal infrared (TIR) canopy temperature.

A. Observed Soil Moisture

Six 7.2-cm diameter soil cores were collected between day 287 and day 290. Their soil moisture contents were measured for 0–2-, 2–4-, 4–6-, 6–8-, and 8–10-cm depth intervals. The average of the 30 moisture content measurements was 34.1% by volume, and the average bound water was 3.5% by volume. The method of estimating average bound water has been discussed by Liou and England [14]. Linear interpolations between the 8–10-cm measurements and 1-m measurements were used for depths below 10-cm. Finally, the observed moisture profiles were approximated with a cubic spline [31].

B. Observed Canopy Moisture

Grass samples were dried at 70°C for nine days. The average dry vegetated column density at the six core sites was 2.28 kg/m^2, and the corresponding average moisture was 1.40 kg/m^2. The total wet biomass of the canopy, 3.68 kg/m^2, was regarded as constant throughout the 14-day simulation period—an acceptable assumption because vegetation maintains its moisture content even as soil moisture varies within relatively broad limits.

C. Canopy Constitutive Properties

Shortwave radioation absorbed by the canopy can be related to LAI by (11), but LAI was not measured at the REBEX-1 site. We estimated LAI from a survey of the literature and the subsequent performance of the 1dH module.

LAI values for a variety of plant species are shown in Table I. Prairie grassland at the REBEX-1 site was denser and taller than grass over the Konza prairie, which had an LAI of 2.18. Based on running the 1dH module with LAI values between two and five, we found the best fit between predictions and observations for an LAI of three. In general, the canopy temperature increases for a given time-of-day with increasing LAI.

TABLE I
OBSERVATIONS OF LAI FOR A VARIETY OF VEGETATION

Plant Type	LAI Range	Investigators
Rice	2.19 ~ 4.97	Shibayama and Akiyama [32]
Rice	1.16 ~ 5.31	Shibayama et al [33]
Wheat	0.39 ~ 2.42	Richardson and Wiegand [34]
Corn	1.33 ~ 3.32	[34]
Cotton	0.42 ~ 3.60	[34]
Sorghum Canopy	3.35	[34]
Konza Prairie	0.12 ~ 2.18	Middleton [35]
Prairie	0.3 ~ 3.0	Verma et al [26]
Alfalfa	3.8	Paloscia and Pampaloni [36]

Verseghy *et al.* [22] found that low values of the minimum canopy resistance to moisture transport ($25 < r_{c,\min} < 100$ s/m) are appropriate for dense, green, unstressed canopies. A higher value of canopy resistance ($r_{c,\min} = 450$ s/m) is appropriate for mature canopies [28]. Our grass was certainly mature and probably senescent. We used an $r_{c,\min}$ of 400.

D. Canopy Albedo

Downwelling longwave radiation, $Q_{l,d}$, an important forcing for the 1dH module, was not measured during REBEX-1. We estimated values for $Q_{l,d}$ from observed downwelling shortwave radiation, net radiation, TIR canopy temperature, and the model-estimated canopy albedo, i.e.,

$$Q_{l,d} = R_{\text{net}}/e_c + \sigma T_c^4 - (1 - A_c)Q_{s,d}/e_c \qquad (39)$$

where

R_{net} observed net radiation, W/m^2;
$Q_{s,d}$ observed downwelling shortwave radiation, W/m^2.

The albedo A_c is the only unknown on the right-hand side of (39). We compared three methods for estimating canopy albedos as follows.

1) We used the spectral reflectance of the canopy at red and near-infrared (NIR) bands combined with the Ahmad and Deering [37] model of reflectance.
2) We used the spectral reflectance of the canopy in the green band by adding 3% to that in the red band % [38].
3) We used the inversion model of Brest and Goward [39] for vegetation.

The maximum and minimum of the computed albedos in the two-week simulation period were 0.40 and 0.20, respectively. While this range of albedos appears to be reasonable [40], [41], we can further test the approach by comparing the consequent estimates of $Q_{l,d}$ with predictions from models by Brutsaert [42], Satterlund [43], and Kahle [44]

$$\begin{aligned} Q_{l,d} &= 1.24\sigma T_a^4(100e_v/T_a)^{1/7} \text{ [42]} \\ Q_{l,d} &= 1.08\sigma T_a^4(1 - e^{-e_v T_a/20.16}) \text{ [43]} \\ Q_{l,d} &= \sigma T_a^4(0.61 + 0.004\,33\sqrt{e_v \text{RH}_a}) \text{ [44]} \end{aligned} \qquad (40)$$

where

e_v water vapor pressure, Pa;
T_a air temperature at screen height, K;
RH_a air relative humidity.

TABLE II
THE AD AND S.D. FROM COMPARISONS BETWEEN THE MODEL-PREDICTED $Q_{l,d}$ AND REFERENCE CASES WITH ALBEDOS OF 0.1 AND 0.4

	Albedo = 0.1		Albedo = 0.4	
Method	AD, W/m^2	SD, W/m^2	AD, W/m^2	SD, W/m^2
Brutsaert [42]	-14.5	98.8	-51.0	103.4
Satterlund [43]	-36.5	144.9	-72.9	162.8
Kahle [44]	-16.4	99.8	-53.0	106.5
1dH/R	16.5	32.9	-20.0	40.1

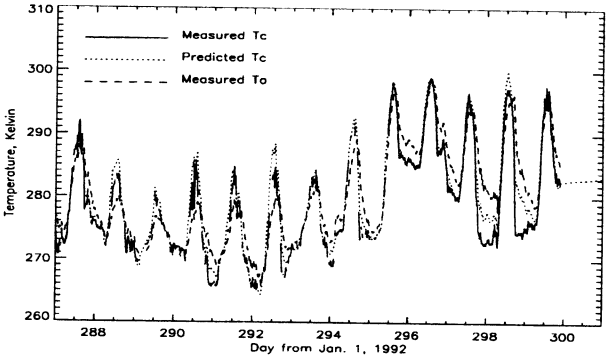

(a)

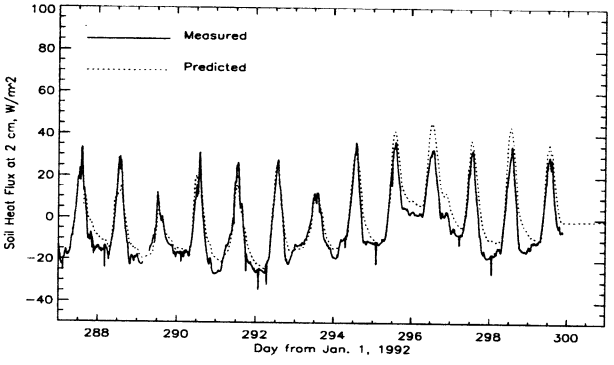

(b)

Fig. 4. (a) Measured canopy and air temperatures and predicted canopy temperature. (b) Measured and predicted soil heat fluxes at 2-cm depth (October 13–26, 1992).

Two limiting cases bound the downwelling longwave radiation—an albedo of 0.1 is certainly a lower limit of $Q_{l,d}$, and an albedo of 0.4 is certainly an upper limit. Table II lists the average of the differences (AD) and standard deviation (s.d.) between the model-predicted downwelling longwave radiation and $Q_{l,d}$ obtained with albedos of 0.1 and 0.4.

The AD values are all negative, and the s.d. are large for the Satterlund [43], Brutsaert [42], and Kahle [44] models. The s.d. values from the 1dH module are smaller, and the AD values are positive and negative for the lower and upper limits of albedo, respectively. That is, among these possible approaches for estimating $Q_{l,d}$, the 1dH-based estimates for $Q_{l,d}$ are at least consistent.

Fig. 4 shows measured and predicted canopy temperatures and measured air temperatures. Predicted canopy temperatures agree with the measured temperatures, except for 2–3-K differences near diurnal maxima on days 288, 292, and 298. The diurnal variation is generally larger for canopy temperature

than for air temperature as expected because it is primarily the canopy that heats and cools the air. The AD and s.d. of the model-predicted versus measured canopy temperatures are 1.1 K and 1.9 K, respectively.

Fig. 4(b) shows that the 14-day modeled soil heat flux at 2-cm depth initially converges to the measured heat flux. The model begins to overestimate the soil heat flux around day 295. These increasing differences may be caused by accumulated model errors from sources like poor initialization of soil layers below 10 cm, approximations with shortwave transmissivity model (11), or model-estimated downwelling longwave radiation. Although the predictions and observations diverge, the difference is only a few watts per square meter. The AD between the predicted and measured soil heat fluxes is 4.6 W/m^2, and the corresponding s.d. is 6.9 W/m^2.

Fig. 5 shows the 14-day soil temperatures at 2-, 4-, 8-, 16-, 32-, and 64-cm depths. The small overestimates in soil temperature are associated with overestimates of net downward heat flux. The AD and s.d. are listed in Table III. Both AD and s.d. decrease with depth because of the constant energy and moisture flux constraints at the lower boundary.

E. Radiobrightness

Fig. 6(a) and (b) show predicted 1.4 GHz and measured and predicted 19- and 37-GHz horizontally polarized brightnesses. Predicted and measured 19-GHz brightnesses match very well. Differences occur when the corresponding canopy temperature differences are large. The AD between predicted and measured 19-GHz brightnesses is -0.06 K. The corresponding s.d. is 1.1 K. The 1dH/R model overestimates 37-GHz brightness by 6.0 K (AD) probably because the R module does not include scatter darkening. The 37-GHz s.d. is 2.5 K.

IV. Simulation of a 60-Day Dry-Down

The performance of the 1dH/R model during the REBEX-1 validation encouraged us to proceed with 60-day dry-down simulations in summer to examine the sensitivity of radiobrightness to soil moisture in prairie grassland. The simulation differed from the validation study in the following two respects: First, the model was driven by climatological data, as discussed in Liou and England [14], [15], and second, the initial conditions were changed as follows.

1) Soil moisture was initialized to be a uniform profile of 38% volume moisture.
2) Soil temperature profile for a starting date of June 23 was obtained from the annual thermal model by Liou and England [14].
3) Initial canopy temperature was assumed to be the climatological air temperature for June 23.
4) Minimum canopy resistance was chosen to be 200 s/m, which is half the 400 s/m used in the model validation [28], [22].
5) Reflected downwelling microwave sky brightness is a negligible factor for relatively dense grass and was ignored.

We compare the predictions from the 1dH/R 60-day dry-down simulation for prairie grass with those from the 1dH/R model for bare soils [15]. We also examine the feasibility of using the RTI measure of soil moisture in prairie grassland.

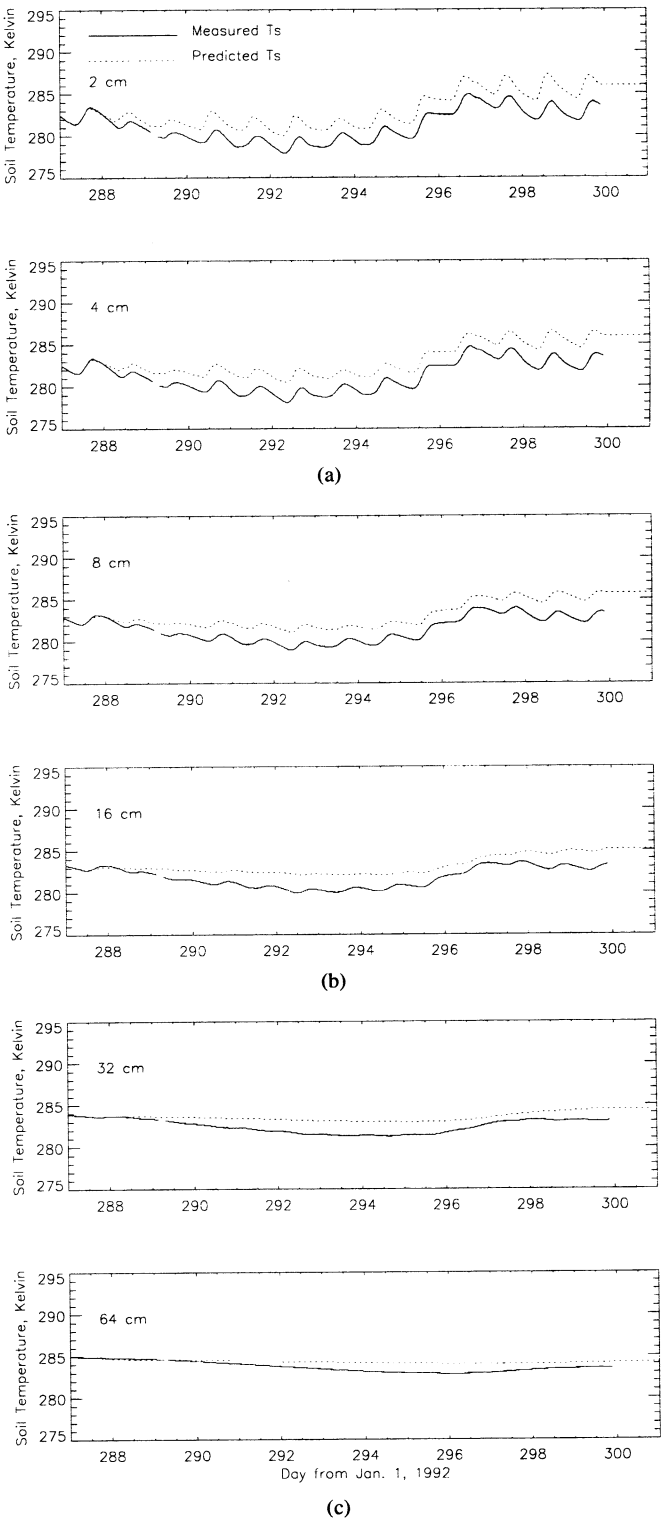

Fig. 5. Soil temperatures at 2-, 4-, 8-, 16-, 32-, and 64-cm depths (October 13–26, 1992).

A. Thermal and Hydrology Signatures

Fig. 7(a) shows the surface moisture content over the 60-day period for both the prairie and the bare soil cases. For bare soil, the surface moisture content exhibited small diurnal

TABLE III
AD AND s.d. BASED ON COMPARISONS BETWEEN MEASURED- AND PREDICTED-SOIL TEMPERATURES

Depth	AD, K	SD, K
2 cm	1.9	2.1
4 cm	1.8	2.0
8 cm	1.6	1.7
16 cm	1.3	1.5
32 cm	1.1	1.2
64 cm	0.6	0.8

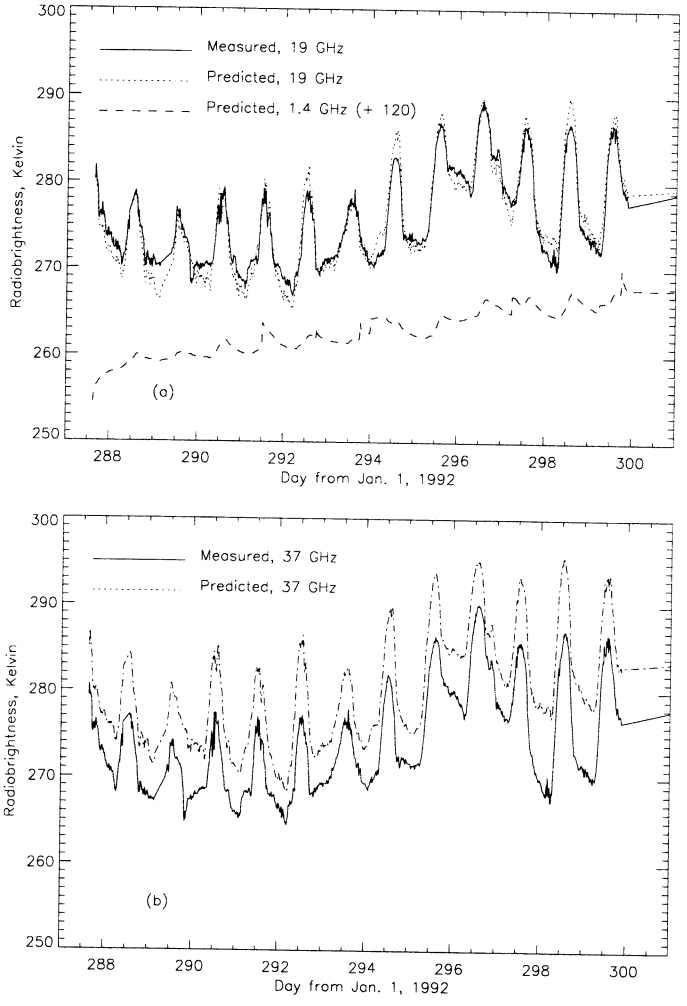

Fig. 6. Comparisons between measured and predicted horizontally polarized brightnesses at (a) 19 GHz and (b) 37 GHz.A plot of predicted horizontally polarized brightness at 1.4 GHz (displaced + 120 K) is included in (a).

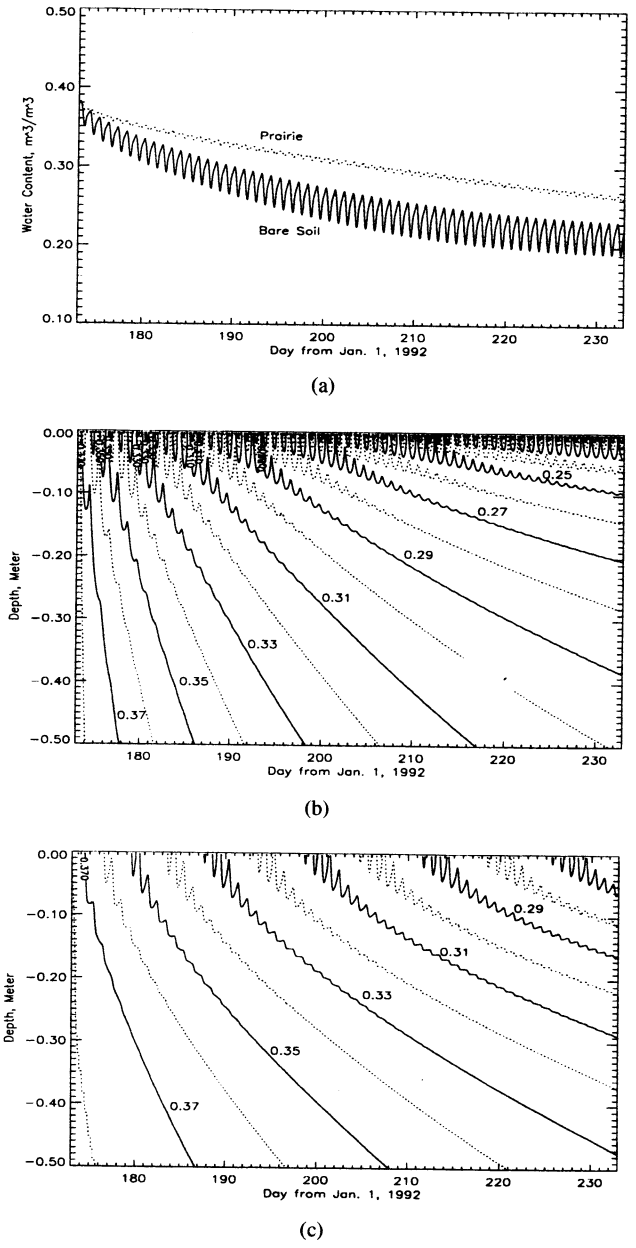

Fig. 7. (a) Soil moisture content at the surface for the prairie grassland and bare soil cases. (b) Soil moisture profile for the bare soil case. (c) Soil moisture profile for the prairie grassland case (June 22–August 21, 1992).

oscillations with a rapidly decreasing average. Diurnal peaks appeared during nighttime due to condensation, and valleys appeared during daytime due to evaporation. For prairie grassland, surface soil moisture remained almost constant over a diurnal cycle and decreased more slowly with daynumber than it did for bare soil. At the end of the 60-day simulation, the decrease in surface soil moisture was 17% for bare soil, but only 11% for grassland. The diurnal variation in surface soil moisture was much larger for bare soil (~4%) than for grassland (~0.5%).

Fig. 7(b) and (c) show constant moisture curves as a function of depth and day number for the 60-day period for bare soil and prairie grassland, respectively. The two figures show increased resistance to latent heat transfer from soil to air for the grassland and more rapid downward propagation of the constant moisture curves for bare soil. Both cases exhibit an expected long-term moisture loss at the surface and a net upward movement of water in the soil and across the land–air boundary.

Soil surface temperatures for prairie grassland and bare soil are shown in Fig. 8(a) and (b), respectively. The weak diurnal oscillation remains almost constant at about 5 K for the prairie grassland case during the 60-day simulation period. The difference in surface temperatures between prairie grassland and bare soil appears to be a moderate diurnal oscillation of 12–16 K resulting from the insulating properties of the vegetation.

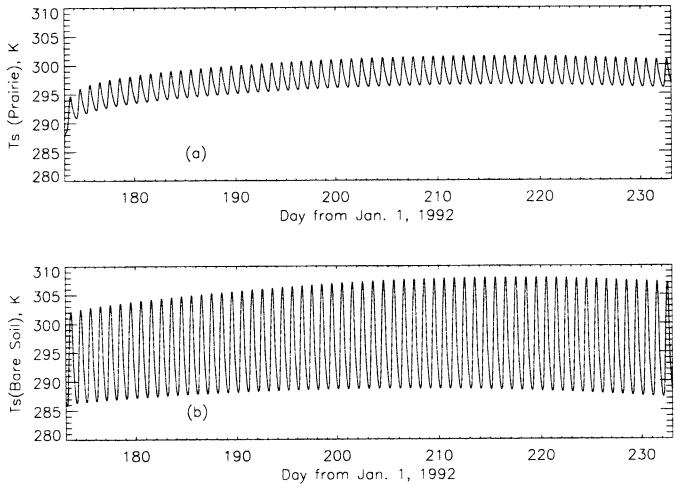

Fig. 8. Surface temperature for (a) prairie grassland and (b) bare soil (June 22–August 21, 1992).

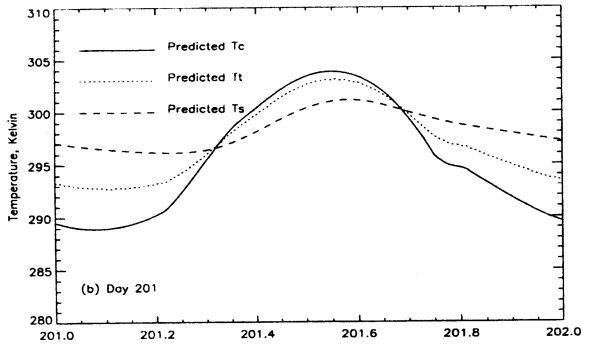

Fig. 9. Temperature for the canopy, thatch, and surface on day 201 (July 20, 1992).

Fig. 9 shows the temperatures for the canopy, thatch, and surface on day 201. The diurnal variations in temperature are approximately 15, 10, and 5 K, respectively, and are typical for the 60-day simulations.

B. Radiobrightness

Fig. 10(a) shows the predicted horizontally polarized brightnesses at 1.4, 19, and 37 GHz versus daynumber for prairie grassland. We observe three characteristics. First, brightnesses at 19 and 37 GHz exhibit diurnal oscillations with a nearly constant average. Second, L-band brightnesses exhibit diurnal oscillations with an average that increases from 143 K at the beginning of the dry-down to 163 K at its end. Third, the amplitudes of the diurnal oscillations in radiobrightness are almost constant throughout the 60-day period, about 3 Kelvins for L-band, 8 K at 19 GHz, and 11 K at 37 GHz. Fig. 10(b) is the equivalent of Fig. 10(a), except that the 1.4-, 19-, and 37-GHz brightnesses are plotted against soil moisture.

Fig. 10(c) shows the percentage of 1.4-, 19-, and 37-GHz brightnesses that originates in the soil. The soil radiobrightness weightings are small for the 19- and 37-GHz cases—about 10% for the former and 3% for the latter. The L-band soil radiobrightness weighting varies from 75% on day 173 to 79% on day 232. That is, vegetation has a small influence on predicted L-band radiobrightness, but the 12% decrease in near-surface moisture causes an increase in L-band brightness of 20 K.

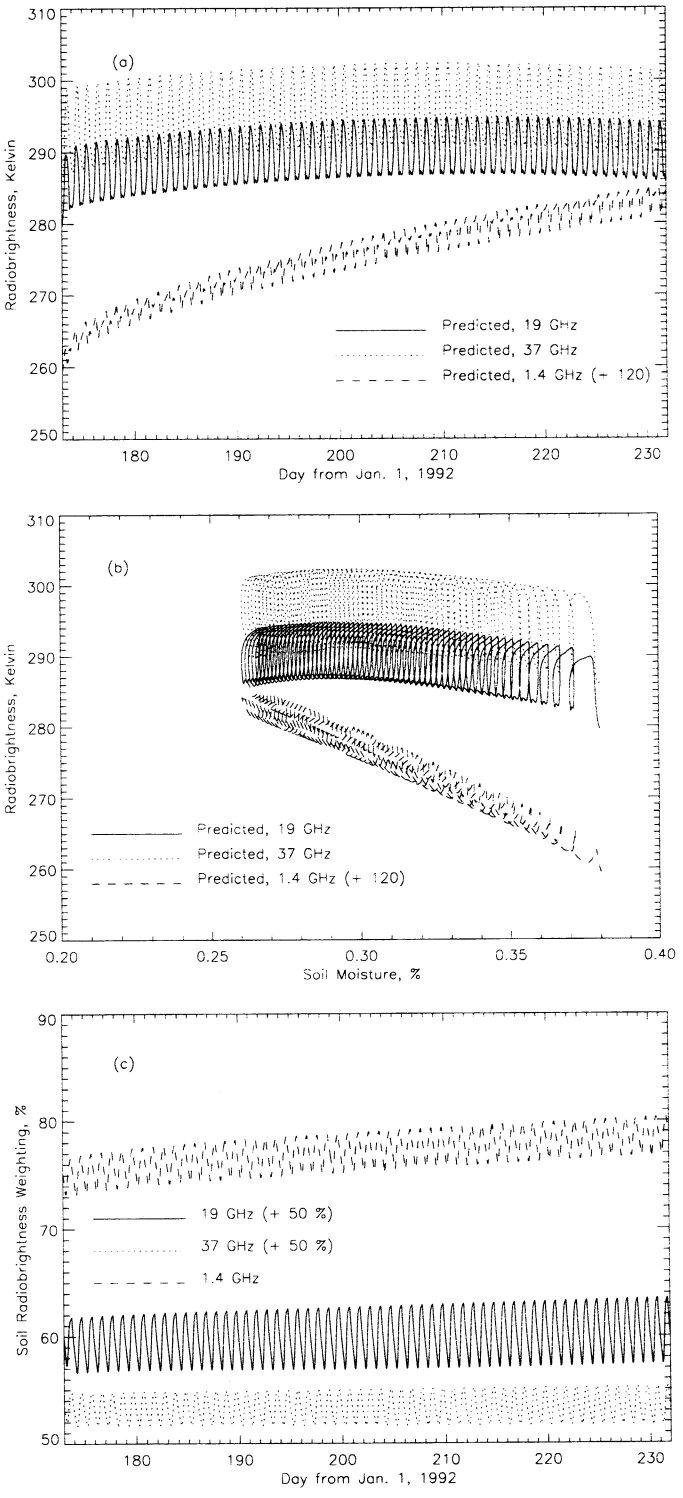

Fig. 10. Horizontally polarized brightnesses at 1.4 (shifted +120 K to ease comparison with 19- and 37-GHz brightnesses), 19, and 37 GHz (a) versus daynumber and (b) versus soil moisture for the grassland case. (c) The percentage of radiobrightness contributed by the soil (June 22–August 21, 1992).

Radiobrightness thermal inertia (RTI) [45] estimates of soil moisture are based on the difference between 2 p.m. and 2 a.m.

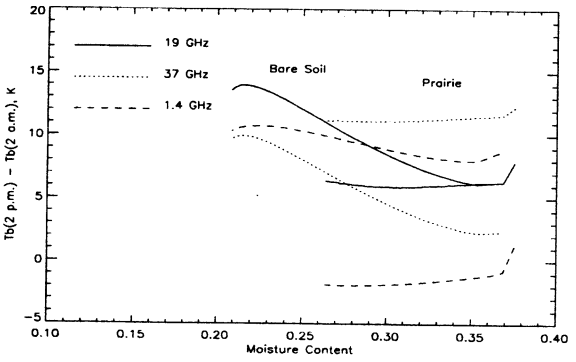

Fig. 11. Differences in radiobrightness between 2 p.m. and 2 a.m. versus soil moisture for bare soil and prairie grassland.

brightnesses for both bare soil and prairie grassland. These differences are shown in Fig. 11. For bare soil, the differences are 7 K at both 19 and 37 GHz. The corresponding change in soil moisture is 16%. The difference at L-band is only 3 K. The L-band emission comes from a greater depth in the moist soil where the diurnal temperature extremes are suppressed. That is, RTI at L-band is less sensitive to surface soil moisture in bare soils than are 19- and 37-GHz brightnesses.

RTI is not sensitive to surface soil moisture in prairie grassland at any of the three frequencies. The 19- and 37-GHz emission from soil does not penetrate the grass canopy. While 1.4-GHz soil emission does penetrate the canopy, the insulating properties of the canopy greatly suppress the diurnal variations in soil temperature.

V. Discussion

The 1dH/R model has been validated for prairie grassland, and although it may be too computationally intensive to be incorporated into an operational weather prediction model, it can be used as a noninteractive model to check estimates of stored water at selected grid points. Comparisons between predicted and observed radiobrightnesses for these points would become a measure of the quality of the stored water estimate.

Our 60-day dry-down simulations showed that L-band radiometry is highly sensitive to surface soil moisture for grass having column densities as high as 3.7 kg/m^2. L-band brightness increased 20 K in response to an 11% decrease in soil moisture. While the special sensor microwave/imager (SSM/I) frequencies of 19, 37, and 85 GHz were sensitive to moisture in bare soil, they were not sensitive to soil moisture in the grassland. Observed moisture sensitivity in SSM/I images of prairie must be a result of mixed-pixel effects of emission from bare or sparsely vegetated areas within each SSM/I pixel. Clearly, estimates of surface soil moisture from brightness must be based on mixed-pixel land-cover models.

Acknowledgment

The authors thank T. Schmugge and the anonymous referees for their suggestions for improving the manuscript.

References

[1] P. R. Rowntree and J. R. Bolton, "Simulation of the atmospheric response to soil moisture anomalies over Europe," *Q. J. R. Meteorol. Soc.*, vol. 109, pp. 501–526, 1983.

[2] W. M. Cunnington and P. R. Rowntree, "Simulation of the Saharan atmosphere-dependence on moisture and albedo," *Q. J. R. Meteorol. Soc.*, vol. 112, pp. 971–999, 1986.

[3] D. P. Rowell and C. Blondin, "The influence of soil wetness distribution on short-range rainfall forecasting in the West African Sahel," *Q. J. R. Meteorol. Soc.*, vol. 116, pp. 1471–1485, 1990.

[4] R. E. Dickinson, A. Henderson-Sellers, P. J. Kennedy, and W. F. Wilson, "Biosphere-atmosphere transfer scheme (BATS) for the NCAR community climate model," Nat. Cent. Atmos. Res., Boulder, CO, Tech. Note NCAR/TN–275+STR, 1986.

[5] P. J. Sellers, Y. Mintz, Y. C. Sud, and A. Dalcher, "A simple biosphere model (SiB) for use within general circulation models," *J. Atmos. Sci.*, vol. 43, pp. 505–531, Mar. 1986.

[6] Y. Xue, P. J. Sellers, J. L. Kinter, and J. Shukla, "A simplified biosphere model for global climate studies," *J. Clim.*, vol. 4, pp. 345–364, Mar. 1991.

[7] J. R. Wang and T. J. Schmugge, "An empirical model for the complex dielectric permittivity of soils as a function of water content," *IEEE Trans. Geosci. Remote Sensing*, vol. GE-18, pp. 288–295, Oct. 1980.

[8] M. C. Dobson, F. T. Ulaby, M. T. Hallikainen, and M. A. El-Rayes, "Microwave dielectric behavior of wet soil—Part II: Dielectric mixing models," *IEEE Trans. Geosci. Remote Sensing*, vol. GE-23, pp. 35–46, Jan. 1985.

[9] M. Hallikainen, F. T. Ulaby, M. C. Dobson, M. El-Rayes, and L.-K. Wu, "Microwave dielectric behavior of wet soil—Part I: Empirical models and experimental observations," *IEEE Trans. Geosci. Remote Sensing*, vol. GE-23, pp. 25–34, Jan. 1985.

[10] T. J. Schmugge, P. E. O'Neill, and J. R. Wang, "Passive microwave soil moisture research," *IEEE Trans. Geosci. Remote Sensing*, vol. GE-24, pp. 12–22, Jan. 1986.

[11] T. J. Jackson and R. E. O'Neill, "Attenuation of soil microwave emission by corn and soybeans at 1.4 and 5 GHz," *IEEE Trans. Geosci. Remote Sensing*, vol. 28, pp. 978–980, Sept. 1990.

[12] World Meteorological Organization, *Scientific Plan for the Global Energy and Water Cycle Experiment*, vol. WCRP-40, WMO-TD 376, 1990.

[13] ———, *Scientific Plan for the GEWEX Continental-Scale International Project (GCIP)*, vol. WCRP-67, WMO-TD, 1992.

[14] Y.-A. Liou and A. W. England, "Annual temperature and radiobrightness signatures for bare soils," *IEEE Trans. Geosci. Remote Sensing*, vol. 34, pp. 981–990, July 1996.

[15] ———, "A land surface process/radiobrightness model with coupled heat and moisture transport in soil," *IEEE Trans. Geosci. Remote Sensing*, vol. 36, pp. 273–286, Jan. 1998.

[16] ———, "A land surface process/radiobrightness model with coupled heat and moisture transport for freezing soils," *IEEE Trans. Geosci. Remote Sensing*, vol. 36, pp. 669–677, Mar. 1998.

[17] J.-F. Mahfouf, "Analysis of soil moisture from near-surface parameters: A feasibility study," *J. Appl. Meteorol.*, vol. 30, pp. 1534–1547, 1991.

[18] F. Bouttier, J.-F. Mahfouf, and J. Noilhan, "Sequential assimilation of soil moisture from atmospheric low-level parameters. Part I: Sensitivity and calibration studies," *J. Appl. Meteorol.*, vol. 32, pp. 1335–1351, Aug. 1993.

[19] V. Lakshmi, E. F. Wood, and B. J. Choudhury, "A soil–canopy-atmosphere model for use in satellite microwave remote sensing," *J. Geophys. Res.*, vol. 102, pp. 6911–6927, 1997.

[20] J. F. Galantowicz, "Field data report for the first radiobrightness energy balance experiment, (REBEX-1), Oct. 1992–Apr. 1993, Sioux Falls, South Dakota," A. W. England, Principal Investigator, UM Radiation Lab. Tech. Rep. RL-913, Feb. 1995.

[21] A. W. England and J. F. Galantowicz, "Observed and modeled radiobrightness of prairie grass in early fall," in *Proc. IGARSS'95 Symp.*, Florence, Italy.

[22] D. L. Verseghy, N. A. McFarlane, and M. Lazare, "CLASS—A Canadian land surface scheme for GCM's. II. Vegetation model and coupled runs," *Int. J. Climatol.*, vol. 13, pp. 347–370, 1993.

[23] P. Dahl, J. Judge, J. Gallo, and A. W. England, "Vertical distribution of biomass and moisture in a prairie grass canopy," UM Radiation Lab. Tech. Rep. RL-902, Nov. 1993.

[24] K. E. Trenberth Ed., *Climate System Modeling*. Cmbridge, U.K.: Cambridge Univ. Press, 1992, pp. 454–457.

[25] A. Chehbouni, E. G. Njoku, J.-P. Lhomme, and Y. H. Kerr, "Approaches for averaging surface parameters and fluxes over heterogeneous terrain," *J. Clim.*, vol. 8, pp. 1386–1393, 1995.
[26] S. B. Verma, J. Kim, and R. J. Clement, "Momentum, water vapor, and carbon dioxide exchange at a centrally located prairie site during FIFE," *J. Geophys. Res.*, vol. 97, pp. 18 629–18 639, Nov. 1992.
[27] J. R. Philip and D. A. de Vries, "Moisture movement in porous materials under temperature gradients," *Trans. Amer. Geophys. Union*, vol. 38, pp. 222–232, Apr. 1957.
[28] J. Noilhan and S. Planton, "A simple parameterization of land surface processes in meteorological models," *Mon. Weath. Rev.*, vol. 117, pp. 536–549, 1989.
[29] B. Jacquemin and J. Noilhan, "Sensitivity study and validation of land surface parameterization using the HAPEX-MOBILHY data set," *Bound.-Layer Meteorol.*, vol. 52, pp. 93–134, 1990.
[30] F. T. Ulaby and M. A. El-Rayes, "Microwave dielectric spectrum of vegetation—Part II: Dual-dispersion model," *IEEE Trans. Geosci. Remote Sensing*, vol. GE-25, pp. 550–557, Sept. 1987.
[31] W. H. Press, B. P. Flannery, S. A. Teukolsky, and W. T. Vetterling, *Numerical Recipes (FORTRAN)*. Cambridge, U.K.: Cambridge Univ. Press, 1989.
[32] M. Shibayama and T. Akiyama, "Seasonal visible, near-infrared and mid-infrared spectra of rice canopies in relation to LAI and above-ground dry phytomass," *Remote Sens. Environ.*, vol. 27, pp. 119–127, 1989.
[33] M. Shibayama, W. Takahashi, S. Morinaga, and T. Akiyama, "Canopy water deficit detection in paddy rice using a high resolution field spectroradiometer," *Remote Sens. Environ.*, vol. 45, pp. 117–126, 1993.
[34] A. J. Richardson and C. L. Wiegand, "Canopy leaf display effects on absorbed, transmitted, and reflected solar radiation," *Remote Sens. Environ.*, vol. 29, pp. 15–24, 1989.
[35] E. M. Middleton, "Solar zenith angle effects on vegetation indices in tallgrass prairie," *Remote Sens. Environ.*, vol. 38, pp. 45–62, 1991.
[36] S. Paloscia and P. Pampaloni, "Microwave vegetation indexes for detecting biomass and water conditions of agricultural crops," *Remote Sens. Environ.*, vol. 40, pp. 15–26, 1992.
[37] S. P. Ahmad and D. W. Deering, "A simple analytical function for bidirectional reflectance," *J. Geophys. Res.*, vol. 97, pp. 18 867–18 886, Nov. 1992.
[38] Y. Li, T. H. Demetriades-Shah, E. T. Kanemasu, J. K. Shultis, and M. B. Kirkham, "Use of second derivatives of canopy reflectance for monitoring prairie vegetation over different soil backgrounds," *Remote Sens. Environ.*, vol. 44, pp. 81–87, 1993.
[39] C. L. Brest and S. N. Goward, "Deriving surface albedo measurements from narrow band satellite data," *Int. J. Remote Sensing*, vol. 8, pp. 351–367, 1987.
[40] K. J. Ranson, J. R. Irons, and C. S. T. Daughtry, "Surface albedo from bidirectional reflectance," *Remote Sens. Environ.*, vol. 35, pp. 201–211, 1991.
[41] A. M. Hasson, "Radiation components over bare and planted soils in a greenhouse," *Solar Energy*, vol. 44, pp. 1–6, 1990.
[42] W. Brutsaert, "On a derivable formula for long-wave radiation from clear skies," *Water Resour. Res.*, vol. 11, pp. 742–744, 1975.
[43] D. R. Satterlund, "An improved equation for estimating long-wave radiation from the atmosphere," *Water Resour. Res.*, vol. 15, pp. 1649–1650, 1979.
[44] A. B. Kahle, "A simple thermal model of the earth's surface for geologic mapping by remote sensing," *J. Geophys. Res.*, vol. 11, pp. 380–387, Apr. 10, 1977.
[45] A. W. England, J. F. Galantowicz, and M. S. Schretter, "The radiobrightness thermal inertia measure of soil moisture," *IEEE Trans. Geosci. Remote Sensing*, vol. 30, pp. 132–139, 1996.

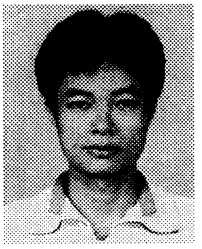

Yuei-An Liou (S'91–M'96) received the B.S. degree in electrical engineering from National Sun Yat-Sen University, Kaohsiung, Taiwan, R.O.C., the M.S.E. degree in electrical engineering, the M.S. degree in atmospheric and space sciences, and the Ph.D. degree in electrical engineering and atmospheric and space sciences from The University of Michigan, Ann Arbor, in 1987, 1992, 1994, and 1996, respectively.

He is currently an Associate Professor at the Center for Space and Remote Sensing Research, National Central University, Chung-Li, Taiwan, R.O.C. From 1989 to 1990, he was a Research Assistant with the National Taiwan University Robotics Laboratory, Taipei. From 1991 to 1996, he was a Graduate Research Assistant at the University of Michigan Radiation Laboratory working in the field of geophysical remote sensing. Since August 1996, he has been with the National Central University. His interests include energy and moisture transport in subsurface porous media, land-atmosphere interactions, microwave radiometric studies of terrains, ocean, and atmosphere, and the coupling of these interactions to atmospheric models.

John F. Galantowicz (S'89–M'95) received the B.S.E. degree in mechanical and aerospace engineering from Princeton University in 1989, and the M.S.E. degree in electrical engineering and the Ph.D. degree in electrical engineering and atmospheric, ocean and space science from the University of Michigan, Ann Arbor, in 1990 and 1995, respectively.

From 1995 to 1997, he was a postdoctoral associate in the Department of Civil and Environmental Engineering, Massachusetts Institute of Technology, Cambridge. In 1997, he joined Atmospheric and Environmental Research, Inc., Cambridge. His current research interests are thermal and microwave remote sensing of land and ice and land–atmosphere interactions.

Dr. Galantowicz is a member of the American Geophysical Union.

Anthony W. England (M'87–SM'89–F'95) received the B.S. and M.S. degrees in earth sciences from the Massachusetts Institute of Technology (MIT), Cambridge, in 1965 and the Ph.D. degree in geophysics from MIT in 1970.

He is a Professor of Electrical Engineering and Computer Science and a Professor of Atmospheric, Oceanic and Space Science at The University of Michigan, Ann Arbor. He teaches electromagnetics and remote sensing geophysics. His research has spanned scattering theory as applied to radio emitters, the development and application of ice-sounding radar for the study of glaciers in Alaska and during two field seasons in Antarctica, and, currently, the assimilation of satellite microwave data in land–surface process models. He was a Scientist/Astronaut during two periods with NASA, where he served on the support crews of Apollo 13 and Apollo 16, flew as a Mission Specialist on Spacelab 2 in 1985, and was Program Scientist for the Space Station during 1986 and 1987. He was a Research Geophysicist and Deputy Chief of the Office of Geochemistry and Geophysics during seven years with the U.S. Geological Survey, and was a Visiting Adjunct Professor at Rice University, Houston, TX, before joining The University of Michigan in 1988. He has been an Associate Editor for the *Journal of Geophysical Research*.

Dr. England is a member of the American Geophysical Union. He has served on the National Research Council's Space Studies Board, and on several federal committees concerned with Antarctic policy, nuclear waste containment, and federal science and technology.